Single-particle dynamics in fluid hydrogen and deuterium

2000 J. Phys.: Condens. Matter 12 A139

(http://iopscience.iop.org/0953-8984/12/8A/315)

J. Phys.: Condens. Matter **12** (2000) A139–A145. Printed in the UK PII: S0953-8984(00)07706-7

Single-particle dynamics in fluid hydrogen and deuterium

C Andreani†, P Cipriani‡, D Colognesi§¶ and E Pace‖

† Dipartimento di Fisica ed Istituto Nazionale per la Fisica della Materia (INFM), Università degli Studi di Roma 'Tor Vergata', Via della Ricerca Scientifica 1, 00133 Roma, Italy
‡ Istituto Nazionale per la Fisica della Materia (INFM), Università degli Studi di Roma 'Tor Vergata', Via della Ricerca Scientifica 1, 00133 Roma, Italy
§ Consiglio Nazionale delle Ricerche ed Istituto Nazionale per la Fisica della Materia (INFM), Italy
‖ Dipartimento di Fisica ed Istituto Nazionale di Fisica Nucleare, Università degli Studi di Roma 'Tor Vergata', Via della Ricerca Scientifica 1, 00133 Roma, Italy

Received 10 September 1999

Abstract. Single-particle response functions for liquid D_2 and H_2, obtained from previous inelastic neutron scattering measurements, are compared with an exact quantum calculation for D_2 and a Wentzel–Kramers–Brillouin (WKB) model for D_2 and H_2. The exact and WKB calculations both provide satisfactory descriptions of the experimental response function of these fluids over a wide range of momentum and energy transfers, which spans from the roto-vibrational excitations up to the molecular dissociation regime.

1. Introduction

The dynamics of single particles and the study of related quantities, such as the mean kinetic energy, $\langle E_k \rangle$, and momentum distribution, $n(p)$, are of fundamental scientific interest in a variety of systems: systems of atoms and molecules, in solid and liquid phases, strongly interacting electron systems, and systems of nucleons in atomic nuclei [1]. The most direct experimental technique which probes single-particle dynamics in condensed matter physics is known as deep inelastic neutron scattering (DINS), or neutron Compton scattering, in analogy with the traditional Compton scattering of photons from electrons. The DINS technique, employing incident neutrons with eV energies, allows one to access high energy, $\hbar\omega > 1$ eV, and a wide range of momentum, 30 Å^{-1} $< q <$ 150 Å^{-1}, transfers. Within the limit of the impulse approximation [2] (IA), the experimental response function $F(y)$ (y is the West scaling variable) [3] is directly related to $n(p)$ for the target system in the initial state. In the case of diatomic molecular systems, the IA relies on two basic assumptions: (1) the scattering is totally incoherent when $q \gg 2\pi/d$, where d is the average intramolecular distance; (2) the struck nuclei recoil under free dynamic conditions when $\hbar\omega$ greatly exceeds the energy scale of internal excitations of the molecule. However, at the intermediate experimentally accessible values of q (and $\hbar\omega$), deviations from the IA can occur, even when the incident neutron energies are larger then 1 eV, as has been discussed in detail in references [4–7].

The aim of the present work is to investigate the q-dependence of the response function, $F(y, q)$, and its asymptotic limit at high q, $F(y)$, for fluid H_2 and D_2. In a previous paper [5] the experimental response functions of these two fluids have already been compared with the

¶ Permanent address: ISIS Facility, Rutherford Appleton Laboratory, Chilton, Didcot, Oxon OX11 0QX, UK.

0953-8984/00/SA0139+07$30.00

results of an approximate calculation, employing a WKB semiclassical approximation [6]. This approach achieved a satisfactory physical description of the experimental response function over the whole range of q explored and showed a continuous transition from a distinct roto-vibrational excitation regime to a free-particle one, as q and ω increased [5].

In the present paper, the above study will be completed by calculating $F(y, q)$ using exact eigenfunctions for the relative motion of atoms within these molecules, to check the ability of the exact calculation to produce a description of experimental data and to test the WKB approximation against the exact calculation.

2. Experimental procedure and theory

The experimental measurements on fluid H_2 and D_2 were performed [5] using the inverse-geometry spectrometer eVS, operating at the ISIS Spallation Neutron Source (UK) [8], where incident neutrons, with energies ranging from 1 eV to 10 eV, are available. A nuclear gold foil, strongly absorbing neutrons at the resonance energy $E_0 = 4911$ meV in an energy window of HWHM $\Delta E_0 = 91$ meV, is placed in the secondary-neutron flight path and selects the final energy of the scattered neutrons. The latter are recorded by lithium glass scintillation detectors. The data span a wide region of ω and q with values of q at the recoiling peak, $\bar{q}$, ranging from $\bar{q} = 28.2$ Å^{-1} up to $\bar{q} = 70.4$ Å^{-1} (see table 1). Full details of the experimental set-up and data-analysis procedure are presented in references [5, 8]. We recall that the measurements for the D_2 sample were made with it in a single state, ortho-D_2, with practically just one kind of internal molecular population ($j = 0$), and the data for H_2 were for almost pure para-H_2 ($j = 0$), with a para-H_2 concentration of 96.2% and an ortho-H_2 ($j = 1$) concentration of 3.8% [5].

Table 1. Values of reduced χ^2 obtained for para-H_2 from two different calculations: the semiclassical approximation (WKB) and the intramolecular impulse approximation (IA). The left-hand-side column reports the scattering angle 2θ, and the right-hand-side one represents $\bar{q}$ (see the text).

2θ (deg)	χ^2 (WKB)	χ^2 (IA)	$\bar{q}$ (Å^{-1})
35.9	0.97	10.2	35.2
37.9	0.75	9.49	38.0
40.0	0.59	6.12	40.8
42.1	0.67	6.98	44.0
44.1	0.83	6.23	47.2
46.1	0.62	5.15	50.6
48.2	0.66	6.22	54.5
50.1	0.96	2.71	58.2

In a DINS experiment at high q, one can neglect the interference terms in the inelastic differential cross section, coming from neutrons scattered by different diatomic molecules [2], and because of the mainly isotropic nature of both the hydrogen and the deuterium intermolecular potentials, it is possible to assume a complete decoupling between intramolecular and intermolecular degrees of freedom [9]. Then the inelastic neutron cross section can be written as a convolution of two terms:

$$\left(\frac{\mathrm{d}^2\sigma}{\mathrm{d}\Omega\,\mathrm{d}\omega}\right) = \int_{-\infty}^{\infty} \mathrm{d}\omega'\, S_{cm}(q, \omega - \omega')\left(\frac{\mathrm{d}^2\sigma}{\mathrm{d}\Omega\,\mathrm{d}\omega'}\right)_{int} \tag{1}$$

where $S_{cm}(q, \omega)$ is the incoherent inelastic structure factor for the centres of mass of the molecules and the other term is the single-molecule inelastic differential cross section,

describing the scattering from an isolated molecule struck by a neutron. For high q, it is appropriate to express $S_{cm}(q,\omega)$ by means of the intermolecular impulse approximation [2], in terms of the single-molecule momentum distribution, $N(\vec{k})$, which is generally assumed to have a Gaussian shape [10] (k is the total-momentum of the molecule). For a molecule with a Gaussian momentum distribution, $S_{cm}(q,\omega)$ also has a Gaussian shape:

$$S_{cm}(q,\omega) = \frac{1}{\sqrt{2\pi\sigma_s^2(q)}} \exp\left\{ -\frac{\left[\omega - \hbar q^2/(4M_1)\right]^2}{2\sigma_s^2(q)} \right\} \tag{2}$$

where

$$\sigma_s^2 = \frac{q^2}{4M_1^2}\sigma_p^2$$

with σ_p^2 the variance [11] of $N(\vec{k})$, and M_1 is the mass of the single atomic nucleus (H or D). In a diatomic molecule, such as H_2 and D_2, because of the isotropy of the interatomic potential, the internal spatial wave function, $\psi(\vec{r})$, can be factorized into radial and angular parts, i.e. $\psi(\vec{r}) = (1/r)u_{v,j}(r)Y_{j,m_j}(\hat{r})$, where v is the radial quantum number and j, m_j are the rotational quantum numbers. Two distinct regimes for the molecule are possible: (i) vibrational states, with the discrete index v of the bound molecule; and (ii) continuum states of the dissociated molecule with v equal to the continuous molecular energy E (the continuum states are degenerate in j). The quantum number j determines the parity, P, of the molecular internal state: $P = (-1)^j$. Then the single-molecule inelastic differential cross section can be written as [5]

$$\left(\frac{\mathrm{d}^2\sigma}{\mathrm{d}\Omega\,\mathrm{d}\omega}\right)_{int} = \frac{k'}{k}\sum_{j'}\sum_{v'(E')}\sum_{j,t} p_{j,t}|a_t^{\pm}|^2 |f_{0,j\to v'(E'),j'}(q)|^2 \delta(\hbar\omega - E_{v'(E'),j'} + E_{0,j}) \tag{3}$$

where $E_{0,j}$ and $E_{v'(E'),j'}$ are the single-molecule initial- and final-state energies, respectively, and $p_{j,t}$ the statistical weights of the initial state (t being the total nuclear spin of the molecule); $|a_t^+|^2$ and $|a_t^-|^2$ are the molecular squared scattering lengths, associated with inelastic transitions between internal states of the same and opposite parity, respectively.

The molecular form factors $|f_{0,j\to v'(E'),j'}(q)|^2$, for the transitions from the initial to the final states, can be expressed in terms of the radial wave functions alone:

$$|f_{0,j\to v'(E'),j'}(q)|^2 = (2j'+1)\sum_{l=|j-j'|}^{j+j'} \left| \int_0^\infty u_{v'(E'),j'}(r)\, j_l(qr/2) u_{0,j}(r)\,\mathrm{d}r \right|^2 \times |\langle j, j', 0, 0|l, 0\rangle|^2. \tag{4}$$

The radial wave functions for the final states have been obtained in two distinct ways: (1) using the WKB approximation; and (2) by an exact solution of the Schrödinger equation for the relative motion of the two atoms in the molecule [5]. In both cases a Morse potential [9] has been assumed to describe the intramolecular interaction. Values used for the potential parameters are reported in reference [5]. The only relevant contribution to the matrix element in a DINS process (equation (4)) comes from the range of r-values where the initial state, $u_{0,j}(r)$ (with $j = 0$, 1 for H_2 and $j = 0$ for D_2), is significantly different from zero [6]. This fact allows one to consider, instead of the exact final radial eigenfunctions, the WKB-approximated wave functions, able to reproduce the correct behaviour in that r-range. For the exact numerical solution, the second-order radial Schrödinger equation

$$\frac{1}{r^2}\frac{\mathrm{d}}{\mathrm{d}r}\left(r^2\frac{\mathrm{d}U}{\mathrm{d}r}\right) = -A[E - V(r)]U(r)$$

has been split into a system of two first-order equations,

$$\frac{\mathrm{d}U}{\mathrm{d}r} = \frac{W}{r^2} \qquad \frac{\mathrm{d}W}{\mathrm{d}r} = -Ar^2[E - V(r)]U(r)$$

which have been solved using a variable increment of the radial coordinate. Indeed the different behaviours of the wave function inside the potential well, i.e. with an increasing number of oscillations as the energy increases, and outside the potential well, i.e. with an exponential decay, suggested the use of a variable increment in order to gain accuracy just inside the potential well, where the wave function is not smooth. Particular care has been taken with the determination of the energy eigenvalues, by checking the continuity of the logarithmic derivatives of 'inner' and 'outer' solutions at both of the classical inversion points, r_1 and r_2 (where $V(r_1) = V(r_2) = E$). The results have been checked for numerical instabilities by changing a control parameter for the variable increment of the radial coordinate.

It is useful to introduce the West scaling variable [3]:

$$y = \frac{M_1}{\hbar^2 q}\left(\hbar\omega - \frac{\hbar^2 q^2}{2M_1}\right)$$

and to describe the scattering response function by the scaling function, $F(y, q)$:

$$F(y, q) = \frac{\hbar q}{2M_1}\left(\frac{\mathrm{d}^2\sigma}{\mathrm{d}\Omega\,\mathrm{d}\omega}\right)\frac{k}{k'}\frac{2\pi}{\sigma_c + \sigma_i} \tag{5}$$

where σ_c and σ_i are the coherent and incoherent scattering cross sections, respectively, of the single nucleus. Numerical values of σ_c and σ_i for H_2 and D_2, as well as of $|a_t^+|^2$ and $|a_t^-|^2$, and the procedure employed for obtaining σ_p^2 can be found in reference [5].

For each single detector, n, at a fixed angle there is a direct correspondence between q and y, $q = q_n(y)$, and one can calculate $F(y, q_n(y))$ along these kinematic curves. In order to perform a comparison with the experimental data, one has to incorporate the contribution coming from the finite resolution function, $R_n(y)$ [7, 12]:

$$F_R(y, q_n(y)) = \int_{-\infty}^{\infty} F(y', q_n(y'))R_n(y - y')\,\mathrm{d}y'. \tag{6}$$

3. Discussion

In order to obtain insight into the changes occurring in the neutron scattering process as a function of energy and q, the functions $F(y, q_n(y))$ (see equation (5)) from the WKB approximation are plotted for H_2, in figure 1, at three distinct scattering angles, together with the results from the intramolecular IA model. In figure 2 the same quantities plus $F(y, q_n(y))$ derived from the exact calculation for D_2 are plotted for three scattering angles. In both figures we observe that $F(y, q_n(y))$ shows, at the lowest angles (see figures 1(a) and 2(a)), a well resolved roto-vibrational structure, more pronounced for the negative y-range, while the response function calculated within the IA model exhibits a quite different form (see figures 1(d) and 2(d)). On increasing the scattering angle (figures 1(b) and 2(b)), a roto-vibrational structure can still be observed for H_2, on the left-hand side of the recoil peak ($y < 0$), while, on the right-hand side ($y > 0$), any structure disappears. Finally, in figures 1(c) and 2(c), exploring the highest-q region (see tables 1 and 2), only a smooth profile remains, both on the left-hand side and on the right-hand side of the recoiling peak. We stress that, in this case, dissociated states of the molecules start to play an important role in the scattering process. From figure 2 it can also be noted that some differences appear between the results obtained using the WKB approximation and from the exact calculation for the highest angles

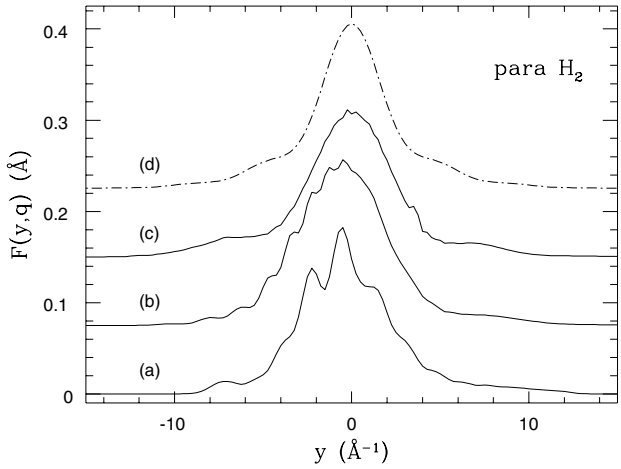

Figure 1. $F(y, q)$ calculated using the WKB approximation for para-H_2 at 17 K for the scattering angles $2\theta = 36^\circ$ (a), $2\theta = 50^\circ$ (b), and $2\theta = 65^\circ$ (c). The response function at the top (d) is from the IA. The response functions (b), (c), and (d) are each vertically shifted by 0.075 Å.

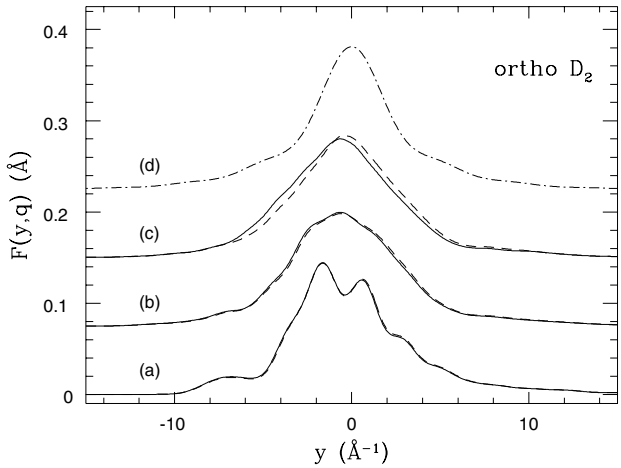

Figure 2. $F(y, q)$ calculated using the WKB approximation (full line) and from the exact calculation (dashed line) for ortho-D_2 at 20.7 K for the scattering angles $2\theta = 39.9^\circ$ (a), $2\theta = 55.5^\circ$ (b), and $2\theta = 70.5^\circ$ (c). The response function at the top (d) is from the IA. The response functions (b), (c), and (d) are each vertically shifted by 0.075 Å.

of the D_2 spectra. These discrepancies show the limit of the WKB approximation as regards coping with final states with high j'-values, as compared to the exact calculation. Indeed as j' grows, due to the increasing centrifugal potential contribution, the classical turning points, poorly described within the WKB, move towards r-values where the initial wave function is significantly different from zero. These discrepancies can be better appreciated by comparing the experimental and calculated $F_R(y, q_n(y))$ (see equation (6)). The latter have been fitted to the experimental response functions in the y-range -20 Å^{-1}–20 Å^{-1}, using a normalization constant as the only free parameter. In the case of H_2, the experimental data were compared only with the WKB and IA results. The reduced χ^2-values obtained from these fits for both fluids are listed in tables 1 and 2, where a satisfactory agreement between experiment and

Table 2. Values of reduced χ^2 obtained for ortho-D_2 from three different calculations: the semiclassical approximation (WKB), the intramolecular impulse approximation (IA), and the exact calculation (EC). The left-hand-side column reports the scattering angle 2θ, and the right-hand-side one represents $\bar{q}$ (see the text).

2θ (deg)	χ^2 (WKB)	χ^2 (IA)	χ^2 (EC)	$\bar{q}$ (Å^{-1})
32.1	1.28	7.03	1.22	28.2
34.7	1.42	8.40	1.30	30.7
37.4	1.30	9.52	1.54	33.4
39.9	1.18	3.46	1.16	35.9
42.5	1.32	5.01	1.31	38.4
45.1	1.30	4.17	1.20	41.1
47.5	1.80	2.96	1.41	43.6
50.1	2.01	2.49	1.55	46.3
55.5	1.29	2.58	1.32	52.3
58.0	1.50	1.78	1.22	55.2
60.6	1.58	1.83	1.31	58.2
63.1	1.27	1.05	1.04	61.1
65.5	2.09	1.20	1.17	64.2
68.0	2.29	1.30	1.79	67.2
70.5	2.11	1.33	1.16	70.4

calculations can be observed. In the case of D_2, the experimental and calculated $F_R(y, q_n(y))$ are also plotted in figure 3 for three selected scattering angles. From this figure and from table 2 we note that the exact calculation provides a quite good description of the experimental data over the whole angular range. Furthermore, at the lowest values of $\bar{q}$ ($\bar{q}$ is the q-value at the recoiling peak, i.e. at $y = 0$), a clear shift of the maximum of the recoiling peak from $y = 0$ can be observed, which dies away as q increases (see figure 3(a)). The smoother shapes of $F_R(y, q_n(y))$ obtained in figure 3, as compared to those of $F(y, q_n(y))$ in figure 2, have to

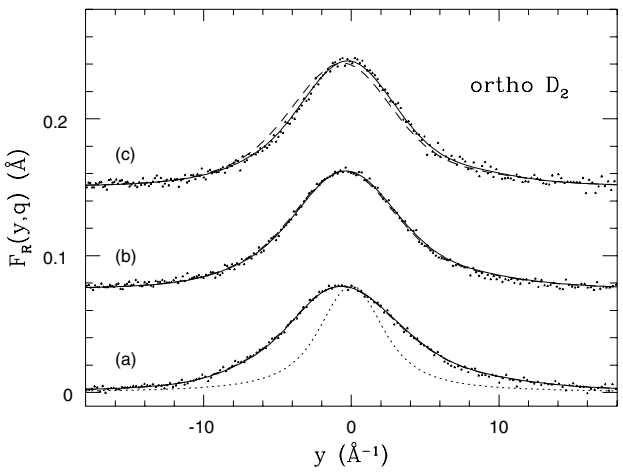

Figure 3. Experimental (points) and calculated $F_R(y, q)$ for liquid deuterium at 20.7 K for the scattering angles $2\theta = 39.9°$ (a), $2\theta = 55.5°$ (b), and $2\theta = 70.5°$ (c); dashed lines are the results of the WKB calculation, and full lines the results of the exact calculation. The resolution contribution (dotted line) is also plotted in (a). The response functions (b) and (c) are each vertically shifted by 0.075 Å.

be ascribed to the convolution of $F(y, q_n(y))$ with the experimental resolution, $R_n(y)$ (plotted in figure 3 as a dotted line for the lowest scattering angle). We stress that, as q increases, the lineshape of the experimental response function in figure 3 reflects a gradual and continuous transition from the roto-vibrational to the molecular dissociation regime, i.e. the superposition of several roto-vibrational molecular excitations and, eventually at high q, a continuum of dissociated molecular states, broadened both by the centre-of-mass motion in the fluid and by the instrumental resolution.

4. Conclusions

DINS experiments on liquid ortho-D_2 and para-H_2 over a wide kinematic region have been compared with theoretical calculations obtained with a Morse functional form for the intramolecular potential. Although the excitation of several roto-vibrational molecular levels occurs, no clear feature of distinct roto-vibrational peaks has been observed experimentally, owing to the present limited resolution of the eVS spectrometer. The eigenfunctions for the internal motion of the two nuclei in the molecule have been obtained within the WKB approximation, or in exact form, by numerically solving the Schrödinger equation. Both calculations satisfactorily reproduce the experimental data over the whole q-range explored, without any free parameter apart from a normalization constant. The exact calculation performs better at the highest values of q, and provides an improvement with respect to other models previously proposed [4, 5, 7, 13].

In conclusion, the WKB approximation is simple and reliable at intermediate values of q, while the IA model, employing plane waves for the final molecular states, is confirmed to be an adequate description of the response function for a liquid system composed of diatomic molecules only for very high values of q.

References

[1] Silver R N and Sokol P E (ed) 1988 *Momentum Distribution* (New York: Plenum)
[2] Lovesey S W 1987 *Theory of Neutron Scattering from Condensed Matter* (Oxford: Oxford University Press)
[3] West G B 1975 *Phys. Rep.* **18** 263
[4] Andreani C, Colognesi D, Filabozzi A, Nardone M and Pace E 1997 *Physica* B **234–236** 329
[5] Andreani C, Colognesi D and Pace E 1999 *Phys. Rev.* B **60** 10 008
[6] Gunn J M F, Andreani C and Mayers J 1986 *J. Phys. C: Solid State Phys.* **19** L835
[7] Andreani C, Colognesi D, Filabozzi A, Pace E and Zoppi M 1998 *J. Phys.: Condens. Matter* **10** 7091
[8] Evans A C, Mayers J, Timms D N and Cooper M J 1993 *Z. Naturf.* a **48** 425
[9] Van Kranendonk J 1983 *Solid Hydrogen* (New York: Plenum)
[10] Sears V F 1985 *Can. J. Phys.* **63** 68
[11] Langel W, Price D L, Simmons R O and Sokol P E 1988 *Phys. Rev.* B **38** 11 275
[12] Andreani C, Baciocco G, Holt R S and Mayers J 1989 *Nucl. Instrum. Methods* A **276** 297
[13] Bafile U, Celli M, Zoppi M and Mayers J 1998 *Phys. Rev.* B **58** 791